

# An introduction to guided and polar surfacing

Jörg Peters, University of Florida,  
Kęstutis Karčiauskas, Vilnius University

April 25, 2009

## Abstract

This paper gives an overview of two recent techniques for high-quality surface constructions: polar layout and the guided approach. We demonstrate the challenge of high-quality surface construction by examples since the notion of surface quality lacks an overarching theory. A key ingredient of high-quality constructions is a good layout of the surface pieces. Polar layout simplifies design and is natural where a high number of pieces meet. A second ingredient is separation of shape design from surface representation by creating an initial guide shape and leveraging classical approximation-theoretic tools to construct a final surface compatible with industry standards, either as a finite number of polynomial patches or as a subdivision process. An example construction generating guided  $C^2$  surfaces from patches of degree bi-3 highlights the power of the approach.

## 1 Introduction

Understanding the notion of a ‘fair’ or high-quality surface and the construction of curvature continuous, parametric surfaces well enough to no longer treat multi-sided blends as a difficult exception is an ongoing research challenge for the community. This paper gives an overview of two useful techniques for constructing high-quality surfaces. Such surfaces satisfy more stringent shape and differential requirements, outlined in Section 2, than might be needed for computer graphics (where speed of construction and rendering, with displacement for detail, is the main challenge) or result from scanning existing artifacts (where compression and manipulation are major challenges).

## 2 The higher-order surfacing challenge

The ability to efficiently design geometrically-high-quality surfaces has a direct impact on better product design and industrial competitiveness. Yet there has been little progress in automating high-quality surface generation. In practice, industry manages by time-consuming human intervention and by rejecting designs that are considered too complex. Regions where several primary surfaces meet are of special concern. Figure 1 shows a C-pillar configuration where a car roof support meets the trunk and

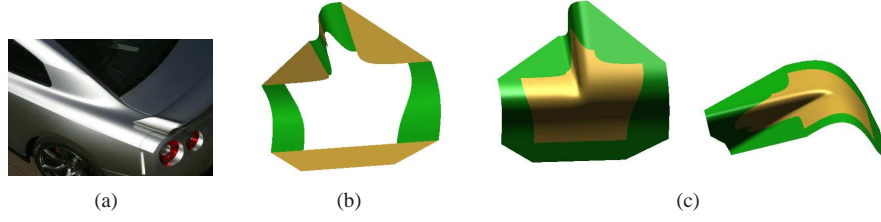


Figure 1: **Multi-sided blend.** (a) Automobile C-pillar, (b) Trimmed primary surfaces pairwise blended. (c) High-quality fill.

fender region. As Figure 1 (b) illustrates, the primary surfaces (light, gold color in the example) are trimmed, then pairwise joined by blend surfaces (darker, green color) leaving a multi-sided hole to be filled in ( see e.g. [VR97]). The quality of the multi-sided fill depends on (i) preserving feature lines and functional curves and (ii) avoiding extraneous dips in the surface so that highlight lines vary smoothly and monotonically almost everywhere. Some car designers additionally check for (iii) undue variation in the curvature by sliding their hand over a first physical prototype of the surface. The multi-sided surface blend of Figure 1 (c) was judged A-class (at General Motors) ‘because our tests did not show anything undesirable’. Short of manufacturing the part, such tests consist of simulating the reflection of parallel light sources, normal and curvature distributions and section curvature (hedgehog) displays on the computer model.

Figure 2 shows some typical shape defects, detected in the computer model, of surfaces generated by standard and more sophisticated blend constructions in the literature. Some of these defects are macroscopic, and immediately visible by computer rendering, while more subtle ones become evident only when applying a Gauss-curvature texture, i.e. color the surface according to Gauss curvature. Example (a) shows the effect of the finite support of the underlying basis functions: a ridge diagonal to the parameter lines of a tensor-product spline results in aliasing ripples. Example (b) shows a similar ripple formation for Loop subdivision [Loo87], where low and high-valent vertices meet (the control net is that of a pinched cylinder and features a central point of valence 20 surrounded by points of valence 3.) Example (c) display a more subtle defect, visible as a pinch-point in the highlight lines. Example (d) illustrates a pervasive problem of first-generation subdivision algorithms for a range of input meshes: the shape is ‘hybrid’, i.e. each nested surface ring of a subdivision surface has both positive and negative Gauss curvature so that the curvature is not well-defined in the limit. This hybrid shape is visualized, for one surface ring, by overlaying on the Bézier net, curvature needles pointed up (red scale, positive Gauss curvature) and down (blue-green scale, negative Gauss curvature). Example (e) illustrates how ‘tuning’ Catmull-Clark subdivision [CC78] to achieve bounded curvature results in oscillation (of the Gauss curvature). The standard Catmull-Clark limit surface has extraordinary points (corresponding to non-4-valent control nodes) with infinite curvature and is generically hyperbolic. Example (f) shows unintended curvature oscillations (Gauss curvature shading) in a transition layer and not consistent with the monotone curvature variation at the center and in the surrounding outer region.

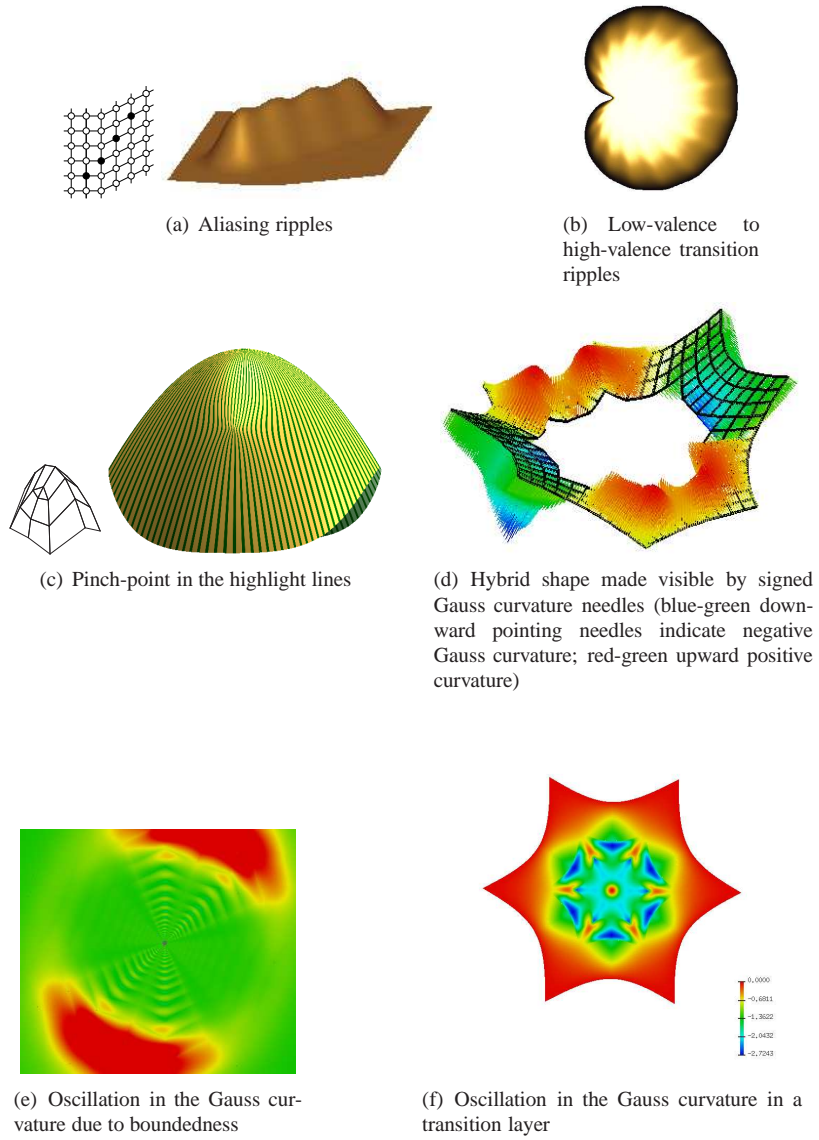


Figure 2: Surface **shape defects**

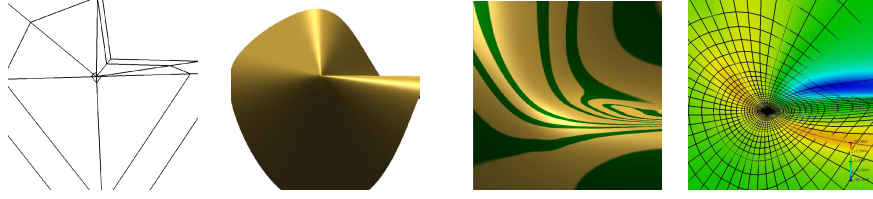



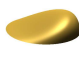
Figure 3: **Feature preservation:** minimal curvature variation and parameter lines aligned with feature lines

Some defects, certainly (a), can be avoided by the experienced designer (by aligning features with boundaries of the support of the basis functions). But [PR04, KPR04] showed that shape deficiency (d) is intrinsic to all first-generation subdivision surface constructions such as the popular Catmull-Clark subdivision [CC78]: While subdivision initially does a fine job in smoothing out transitions between primary surfaces, the shape problems are typically concentrated in the neighborhood of so-called extraordinary points. The surface quality deteriorates progressively as ‘the wrong’ eigenfrequencies take over near such a point, and force for example saddle shapes no matter how carefully a designer might hand-adjust the input data. Since the shape defects manifest themselves already in the first steps, algorithms that build on or initialize with several steps of Catmull-Clark subdivision inherit coarse-level defects. More smoothing of the regular regions [ZS01] appears to be even more detrimental to the shape near these extraordinary points. Conversely, constructions that do not make use of multiple refinement steps and construct the blend from a minimal number of polynomial pieces pay for the abrupt transition of patch type with curvature fluctuations (Figure 2(f)).

Since no overarching theory of surface ‘fairness’ exists to date, we extract from folklore, theory and many examples the following working definition of a high-quality surface blend. Given input data to be matched, a multi-sided surface blend is of *high quality* if it *does not create curvature features not implied by the input data*. That is, the blend surface should (a) minimize curvature variation but (b) preserve feature lines. By default, the blend should therefore be at least curvature continuous. In practice, since many downstream algorithms work directly on the parameterization, we also expect a high-quality surface blend to have (c) a good distribution of parameter lines.

One approach to improving surface quality is to optimize a (variational) functional. Shape optimization functionals include the thin plate energy [BW90, Gre94, HG00, MS92, Sap94, WW92], the membrane energy [KCVS98], and total curvature [KHPS97, WW94]. Replacing differential operators by differences, the optimization problems can be solved as sparse, finite linear or nonlinear systems in the coefficients of a chosen basis. *Evolution* formulations seek to reduce variation which, for a surface  $\mathbf{x}(u, v)$ , amounts to solving the (geometric diffusion) equation  $\partial_t \mathbf{x} = \Delta_{\mathbf{x}} \mathbf{x}$  in terms of the  $\mathbf{x}$ -dependent Laplace-Beltrami operator  $\Delta_{\mathbf{x}}$  [dC92]. Discretized versions of the Laplacian have been applied to polyhedral meshes, say in Taubin’s pioneering paper [Tau95], and, in the context of smoothing interpolatory subdivision and multiresolution editing [Kob97, KCVS98]. Desbrun et al. [DMSB99] use implicit discretization to stabilize numerical smoothing and Clarenz et al. introduced anisotropic geomet-

ric diffusion to enhance features while smoothing. Similar discretizations are based on [MDSB02, PP93]. *Flow techniques* evolve the surface according to  $\partial_t \mathbf{x} = \mathbf{v}(\mathbf{x}, t)$  where  $\mathbf{v}$  represents a velocity field [WJE00, JKL<sup>+</sup>]. For example, geodesic curvature flow has been used for smoothing functions on surfaces [Kim97, MS96, DMSB99]. Schneider and Kobbelt [SK00] distinguish between ‘outer fairness’ and ‘inner fairness’. Outer fairness amounts to satisfying the discretized partial differential equation  $\Delta_{\mathbf{x}} H(\mathbf{x}) = 0$  where  $H$  is the mean surface curvature. Inner fairness seeks a good distribution of parameter lines. The latter is closely related to mapping, with least distortion, a 3D triangulation to the plane [Flo97, SdS00, GGH02]. Thus inner fairness addresses point (c) above; but none of the criteria directly optimizes (a) or (b). Low-order *linear functionals* such as  $\min \int \Sigma(\partial_{ij} \mathbf{x})^2$  are computationally efficient but give preference to polynomial representations of low degree. This restricts shape and can lead to unwanted flatness of the surface. While the above-mentioned geometric diffusion and mean curvature criteria aim in the right direction, such criteria are difficult

to customize to allow a designer to prescribe  rather than . One possible approach to fairing is to leverage advances in difference geometry by generating a *discrete mesh-based* representation first, for example by fairing according to [HP07]. The difficulty is then in switching to a parametric surface since, typically, interpretation of the mesh points by (quasi-)interpolation leads to surface oscillations (see e.g. [KP09c]). Similarly, switching from a level-set representation induced by a scalar field (where application of linear functionals makes sense) to the required parametric output risks losing any of the qualities that the field was optimized for. As an alternative and key element of this survey, Section 4 therefore proposes the use of local shape hints in the form of local (guide) surface fragments.

Generating *curvature continuous surfaces* without focus on surface fairness, on the other hand, is no longer a major challenge. A number of sophisticated algorithms now exist that automatically create curvature continuous blends. Polynomial  $G^2$  blends (where  $G^k$  indicates that adjacent patches’ derivatives agree after reparameterization) include for example [Hah89, GH89, Ye97, Rei98, Rei99, Pra97, Pet96, GZ99, Loo04, LS08, Pet02, KMP06, KP07a, KP07c, KP07b, KP08b, KPN1] for quadrilateral patches and [PU00, BR97, KP07a, KP09a] for triangular patches. Rational  $G^2$  blends include [NG00, GH95] and there are non-polynomial constructions resulting in  $C^2$  surfaces [YZ04, Lev06]. Yet, while local curvature continuity is helpful in analyzing surfaces, it is clearly not sufficient and certainly none of the early constructions can claim to meet both the shape and representation requirements of product-defining outer surfaces in high-end CAD/CAM design (which need to be compatible with the industry’s NURBS standard). Still, spline constructions of everywhere curvature continuous surfaces are now well enough understood to consider them a starting point rather than a goal in themselves. This state of the art sets the stage for this survey’s discussion of two complementary techniques for improving the quality of curvature continuous surfaces.

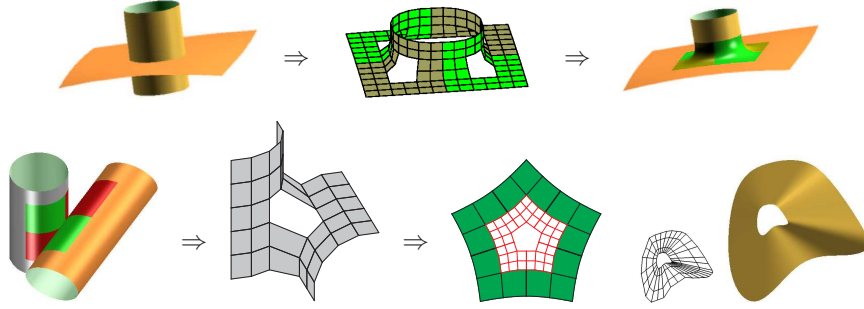


Figure 4: **Trimming and abstraction of boundary data.** (*top*) The set back (trimmed) surfaces are sampled to provide a depth 2 *tensor-border* (spline representation of the boundary) with 5-sided holes. (*bottom*) Tensor-border derived from two cylinders. Such borders then have the same layout as the standard setup of subdivision (*middle*) and (*right*).

### 3 Patch layout

The layout of patches, i.e. the coarse parameterization of the surface, is an art requiring a good understanding of the support and approximation order of the underlying representation (Figure 2 a,b) as well as of conceptual and geometric considerations. Allowing more flexibility in the layout simplifies the layout problem and can improve the shape where a large number of patches join, such as a pole in the latitude-longitude parameterization of the sphere.

The layout typically chosen in the (untrimmed) academic setting is one induced by quadrilateral-based (tensor-product) subdivision surfaces, such as Catmull-Clark subdivision [CC78]; or by triangle-based (three direction box-spline) subdivision, such as Loop's [Loo87]. Setback blending, more typical in industrial design, where primary surfaces are trimmed back and pairwise blended, can be transformed to the subdivision setting by recording the first  $k$  derivatives across the resulting boundary. We call such data along a boundary (loop) a *depth  $k$  tensor-border* (see Figure 4, *middle*).

In either case the multi-sided holes have no corresponding box-spline basis function but are filled, either with a cap of  $n$  (macro-)patches or via subdivision, i.e. by an infinite sequence of surface rings. Fundamentally, there are two types of layouts, depending on whether the edge  $(t, 0)$  or the edge  $(1, t)$  of the domain is mapped to the predecessor's edge  $(0, t)$ . In the first case (Figure 5, *left two*), the layout reminds of a *sprocket*, a mechanical part with gear-teeth. Such a layout is illustrated in Figure 6, *left*. In the vicinity of the  $n$ -valent center this configuration mimics the map  $z^{4/n}, z \in \mathbb{C}$  and for large  $n$ , the parameter lines are increasingly at odds with the curvature lines. Another characteristic of this layout are T-corners. A *T-corner* is the location where an edge between two distinct polynomial patches meets the midpoint of an edge of a third. With each refinement, quad-based sprocket layout subdivision such as Catmull-Clark subdivision generates T-corners between the patches of the new surface ring and its outer ancestor. Generally, nested surface rings of quad-sprocket subdivision rings have a cascading sequence of T-corners (Figure 5, *left*). Similarly, triangle-sprocket subdivi-

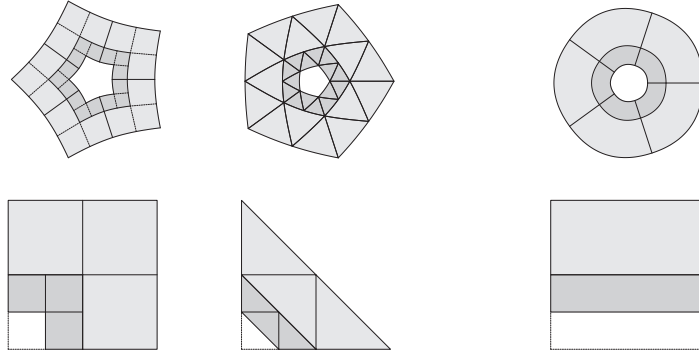


Figure 5: **Layout** (top) Tessellating annuli generated by ct-maps (page 10)  $\rho$  and  $\lambda\rho$  [KP07a]. (bottom) Domains  $S$  and  $S/2$  of each of the  $n = 5$  pieces used for the prolongation  $p(S/2) := \lambda\rho(S)$ . (left) Quad-sprocket (Catmull-Clark subdivision) layout; (middle) Triangle-sprocket (Loop subdivision) layout; (right) polar layout ( $S/2$  is interpreted as halving only the vertical direction).

sion rings have a sequence of points where 5 rather than the standard 6 patches meet and one angle is  $\pi$ .

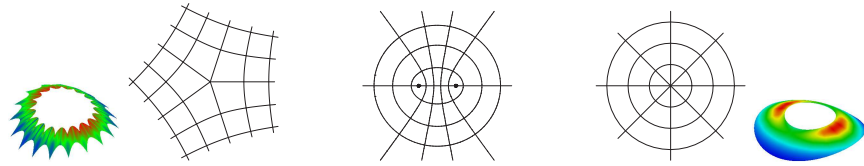


Figure 6: (middle three) Iso-parameter lines of the **conformal** mappings (left)  $z^{4/n}$ ; (middle)  $\cos z$ ; (right)  $e^z$ . (Outer two) Gauss curvature images on a surface ring of (far left) quad- or triangle-sprocket subdivision, (far right) polar subdivision.

An alternative layout for subdivision is the polar layout (Figure 5, *right*) typified by the parameter lines of the map  $e^z$  (Figure 6, *right*). Here the  $n$  bounding spline segments combine to a single spline curve and the central facets are triangles that may be interpreted as quads with one collapsed edge. An intermediate configuration is the double-lens configuration according to the parameter lines of the map  $\cos z = 1 + z^{4/2} + \dots$  mediating between the two extremes [KP09c].

Polar layout allows for surface constructions (both by subdivision or finitely many patches [KP07d]) that thrive on high valences (see Figure 7). Such high valences occur naturally in the design of surfaces of revolution and extruded shapes. Combining sprocket layout and polar layout [MKP08] allows keeping the Catmull-Clark valence low by shifting high-valence connectivity to polar structures and orienting the control lines along model features (e.g. the mouth, nose and eyes in Figure 8).



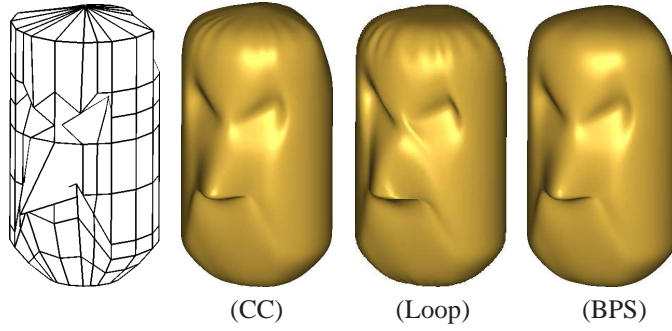


Figure 7: Wrinkle removal by **polar layout** (CC=Catmull-Clark subdivision [CC78], Loop=[Loo87], BPS = Bi-3 polar subdivision [KP07d]).

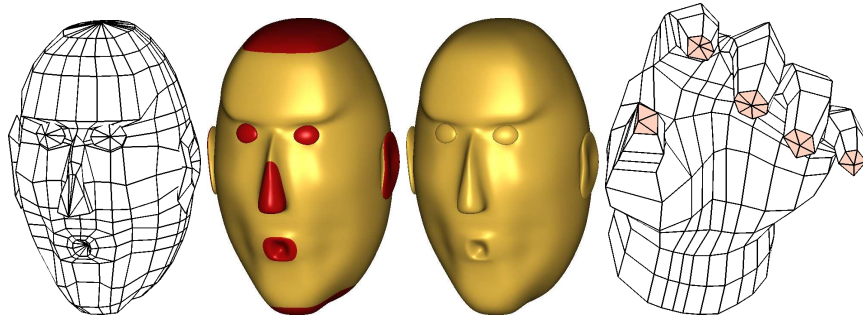


Figure 8: **Combining** polar layout (for high valences, such as the centers of the eyes) with sprocket layout (for low valences, such as the 5-valent vertices surrounding the mouth or between thumb and index finger on the *right*) [MKP07].



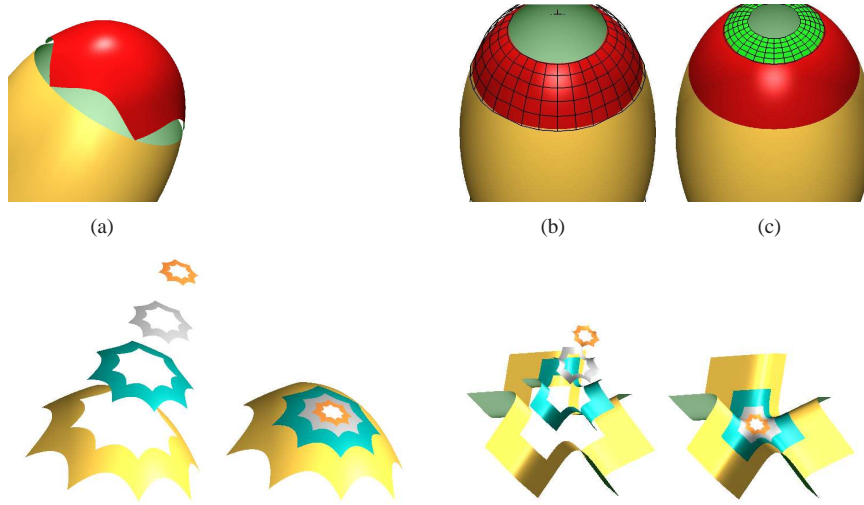


Figure 9: **Guided surface rings.** (*top*) Polar layout. (a) boundary data and guide (red cap) (b) first layer, (c) second layer [KMP06]. (*bottom*) Sprocket layout. The guided rings are shown first in an exploded view, then combined to one surface [KP07a].

## 4 Guided Surfacing

While prior approaches attempted to address both shape design and representation in one step, guided surface construction *separates shape design from surface representation*. In the guided approach, the shape is defined via local surface fragments, called guides, that need only obey few constraints (see Figure 9, *top, left*). A guide typically does not match the boundary data but overlaps or leaves gaps; a guide may be of too high a degree for downstream algorithms (piecewise degree 12 is useful for some configurations) or it may have an otherwise undesirable representation that does not fit into the processing pipeline. Leveraging classical techniques of approximation theory and spline construction, the guide is replaced by a sequence of nested, smoothly joined surface rings so that the output consists of parametric pieces in standard rational or polynomial form. Guide-based algorithms can be chosen so that the final output consists of a few, of many or, in the case of subdivision, of an infinite number of patches. Both finite and subdivision constructions use guided rings to transition to the central point.

### 4.1 Guided Surface Rings

A *guided surface ring* is a low-degree, piecewise polynomial or rational spline approximation to a ring-shaped region of a given surface fragment, called the *guide*. The two reasons to generate guided rings are:

- to capture the shape of a complex guide surface and
- to obtain a smooth, low-degree standard (piecewise polynomial) representation.

The specific approach implemented in [KP07a] is to generate the  $m$ th guided ring  $\mathbf{x}^m$ ,

$$H \left( \begin{array}{c} \text{guide } \mathbf{g} \\ \triangle \times n \rightarrow \mathbb{R}^3 \end{array} \circ \begin{array}{c} \text{ct-map } \rho \\ S \times n \rightarrow \mathbb{R}^2 \end{array} \right)$$

Figure 10: **Guided ring** generation for sprocket layout.

$m = 0, 1, \dots$  by applying an operator  $H$  that approximates (for example position and higher-order derivatives of) a guide surface  $\mathbf{g}$  at parameters defined and weighted by  $\lambda^m$ -scaled copies of a concentric tessellation map  $\rho$  (see Figure 10):

$$\mathbf{x}^m := H(\mathbf{g} \circ \lambda^m \rho): \quad S \times \{1, \dots, n\} \rightarrow \mathbb{R}^3. \quad (1)$$

We explain this in more detail.

**The concentric tessellation map  $\rho$ .** A concentric tessellation map (short: ct-map) maps  $n$  copies of a *sector domain*  $S$  (see Figure 5, *bottom*) to an annulus in the plane:

$$\rho : S \times \{1, \dots, n\} \rightarrow \mathbb{R}^2,$$

so that  $\lambda^m$ -scaled copies of this annulus join without overlap and smoothly as parameterizations to fill a disk around the origin. Characteristic maps of symmetric subdivision algorithms provide a ready source for ct-maps. For example, Figure 5, *top*, shows uniform  $C^2$  ct-maps for three domain types  $S$ . However, the maps can also be chosen non-uniform and unsymmetric. Figure 12, *bottom* (b) shows (the extension of) such a map and illustrates its use. The ct-map relates the domain of the surface rings to that of the guide: it orients and scales higher-order derivatives that the operator  $H$  extracts from the guide surface.

**The operator  $H$ .** The operator  $H$  maps the composition  $\mathbf{g} \circ \rho : S \times \{1, \dots, n\} \rightarrow \mathbb{R}^3$  to a piecewise polynomial surface in  $\mathbb{R}^3$ . Given an intermediate patch  $h(f)$  that matches the derivatives of a given map  $f$  defined on  $S$ ,  $H$  prolongs it so that consecutive rings  $\mathbf{x}^m, \mathbf{x}^{m+1}$  join smoothly (Figure 9) and the outermost ring,  $\mathbf{x}^0$ , smoothly joins the surrounding multi-sided boundary data, the tensor-border. In typical guided surface constructions, *higher-order jets* (collections of derivatives) of the composition  $f := \mathbf{g} \circ \rho$  are well-defined because the rays that form the segment boundaries of the ct-map  $\rho$  match the domain boundaries of the polynomial pieces of the guide  $\mathbf{g}$ . Then, for example the operator  $h := h^{55}$  for tensor-product patches, generates a patch of degree  $(5, 5)$  as follows. For each corner,  $h^{55}$  samples the second order expansion of  $f$ , and converts it to a  $3 \times 3$  group of Bernstein-Bézier coefficients.

$$\begin{array}{ccc} \partial_t^2 f & \partial_s \partial_t^2 f & \partial_s^2 \partial_t^2 f \\ \partial_t f & \partial_s \partial_t f & \partial_s^2 \partial_t f \\ f & \partial_s f & \partial_s^2 f \end{array} \Rightarrow \begin{array}{ccccc} \circ & \circ & \circ & \circ & \circ & \circ \\ \circ & \circ & \circ & \circ & \circ & \circ \\ \circ & \circ & \circ & \circ & \circ & \circ \\ \cdot & \cdot & \cdot & \circ & \circ & \circ \\ \cdot & \cdot & \cdot & \circ & \circ & \circ \\ \cdot & \cdot & \cdot & \circ & \circ & \circ \end{array} \quad (2)$$

By combining the four groups of nine coefficients per corner,  $h^{55}$  defines the  $6 \times 6$  coefficients of a polynomial patch of degree bi-5. Alternatively,  $h$  can be an operator  $h^{33}$  that substitutes, for each bi-5 patch, a  $3 \times 3$  array of bi-3 patches, i.e. a  $C^2$  spline in B-spline form with single knots in the interior and four-fold knots at the boundary [KP08b]. Clearly many other choices for  $h$  are possible.

**Guided patchworks.** Let  $\rho$  be a ct-map and let the guide  $\mathbf{g}$  be defined as

$$\mathbf{g}: \mathbb{R}^2 \rightarrow \mathbb{R}^3, \quad (u, v) \mapsto (x, y, z). \quad (3)$$

The contraction of the smoothly connected annuli  $\{\lambda^m \rho\}_m$  is inherited by the sequence of compositions  $\{\mathbf{g} \circ \lambda^m \rho\}_m$  and the sampled  $C^2$  guided rings  $\mathbf{x}^m := H(\mathbf{g} \circ \lambda^m \rho)$  will join to form a  $C^2$  surface in  $\mathbb{R}^3$  [KP07a, Lemma 4] (as illustrated in Figure 9). There are a number of possible combinations of  $h$  (and hence  $H$ ) and  $\rho$ . For example, guided  $C^2$  quad-sprocket patchworks in [KP07a] use as  $\rho$  the characteristic ring of Catmull-Clark subdivision (Figure 5 *top, left*) and use  $h := h^{66}$ , which samples up to 3rd order and averages coefficients determined by multiple corners. The operator  $h$  samples  $\mathbf{g} \circ \lambda^m \rho$  at the corners of the  $L$ -shaped segment of a quad-sprocket construction. – For a second example, guided triangle-sprocket patchworks use the characteristic ring of Loop subdivision as  $\rho$  and apply an operator  $h^8$  [KP07a] that returns patches of total degree 8. The finite patchworks defined by these combinations of  $\rho$  and  $H$  (and a similar one for polar layout) can reproduce quadratic expansions at the central point. This yields a systematic way to generate  $C^2$  subdivision surfaces, the topic of the next section.

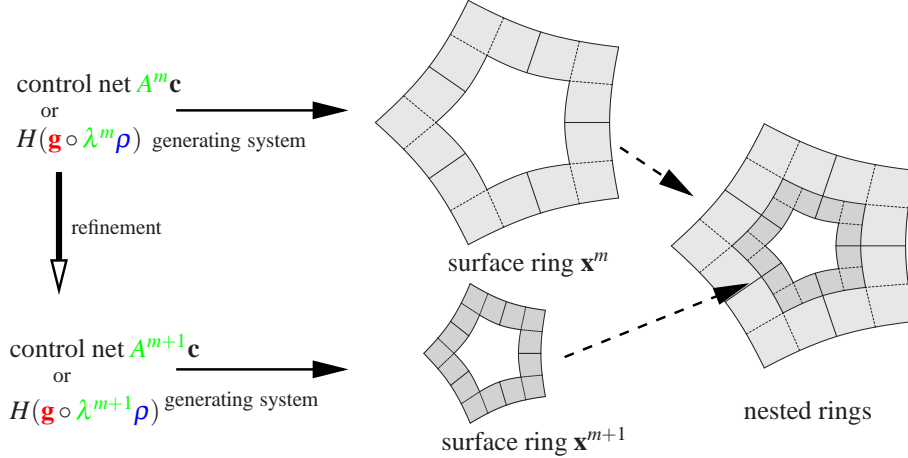


Figure 11: Standard **generalized subdivision** and **guided subdivision** both generate a sequence of nested surface rings: Generalized subdivision surface rings are guided by a subdivision matrix  $A$ , guided subdivision surface rings are guided by an explicit map  $\mathbf{g}$  [KP08b].

## 4.2 Guided Subdivision

A sequence of nested surface rings yields a surface ring structure just like that of standard subdivision (see Figure 11). While standard mesh-based subdivision generates nested surface rings by applying powers of a square subdivision matrix  $A$  to mesh nodes (control points)  $\mathbf{c}$  and interpreting the resulting nodes as, say B-spline control points, guided subdivision composes scaled copies of the ct-map with the guide and then re-approximates to obtain nested surface rings. Indeed the finite union of guided rings is easily constructed to be a  $C^2$  surface. And if the degree of the surface rings is chosen to be bi-6, the guided rings reproduce the quadratic expansion of the  $C^2$  guide at the central point so that the infinite union is  $C^2$  [KP07a, Thm 1]. There are also constructions of degree as low as bi-3 that preserve the shape so that the difference in quality is only visible by comparing Gauss curvature. Figure 10 of [KP08b] shows the correlation of lowering the degree with a deterioration of the curvature distribution (as does the analogous Figure 14 of [KPN1] for finite polynomial constructions).

If the guide is (piecewise) polynomial then the construction of the contracting guided patchwork rings is stationary and guided subdivision has a fast evaluation algorithm based on superposition of eigenfunctions. A specific construction of a  $C^2$  subdivision algorithm without explicit use of the guide is given in [KMP06]. This algorithm maps jets to jets rather than control points in  $\mathbb{R}^3$  to points in  $\mathbb{R}^3$ , of a refined mesh. A general theory of  $C^k$  subdivision constructions analogous to guided subdivision is laid out in [PR08, Ch 7]. Additional images can be found at [Sur].

## 4.3 Construction with finitely many patches

Complex surface blends, for example when capping a  $C^2$  spline surface by  $n$  patches, require an increase in either the degree or the number of pieces compared to the

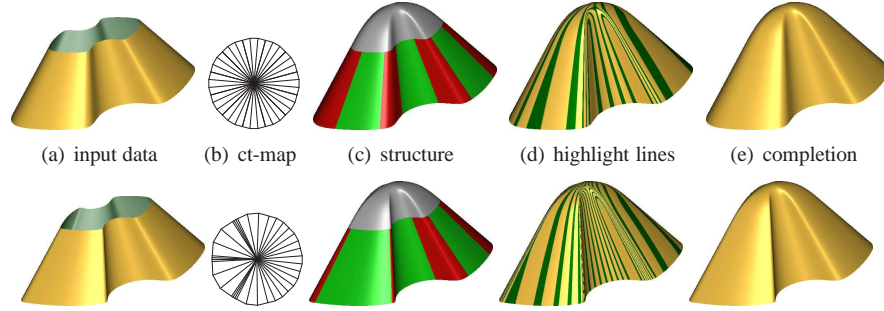


Figure 12: **Completion of a piecewise cone.** Cone pieces (light green) in (c) and pairwise blends (dark red) by  $n$  patches of degree (6,5) (gray) using (*top*) a uniform and (*bottom*) a non-uniform ct-map [KP09b]. The non-uniform ct-map allows us to match the sharper input features on the left lobe.

surrounding regular spline surface. Typically, the new degrees of freedom do not match the formal continuity constraints and this results in an under-constrained problem when fitting with finitely many patches. Guided surfacing effectively localizes the technical

challenges while preserving global shape, even when the number of patches, their layout and/or their degree are high [KP07c, KP07b, KPN1]. Typically, the finite constructions benefit from a few guided rings to transition from the boundary data to the central cap. The guide stabilizes the transition, so that we do not observe the fluctuations of Figure 2 (f). Often, the rings and the final cap can be combined into macro-patches or even splines for implementation. Using such a spline-based approach that trades degree for number of pieces, we recently derived an algorithm for generating  $C^2$  surfaces with sprocket layout consisting of  $n$  splines of degree bi-5 and a finite polar  $C^2$  construction of degree (6,5) [KP09b] (see Figure 12); constructions of even lower-degree are possible for simpler tensor-borders.

#### 4.4 Fitting a Guide

If the design(er) does not provide the guide surface, and/or specifies partial information such as the position and normal of the central point, the following default construction of a piecewise polynomial  $C^2$  guide for sprocket layout can be used [KP09a]. We construct a  $C^2$  map  $\mathbf{g}$  consisting of  $n$  polynomial pieces of total degree 5 (see Figure 13) in BB-form:

$$\mathbf{g}^\ell(u, v) := \sum_{i+j+k=5} \mathbf{g}_{ijk}^\ell \frac{5!}{i!j!k!} u^i v^j (1-u-v)^k, \quad \ell = 1, \dots, n.$$

While there is no restriction on the degree of the guide surface since it is re-sampled and hence does not influence the degree of the output. However, in our experience guide surfaces consisting of  $n$   $C^2$ -connected triangular patches of total degree 5 suffice to approximate well second order boundary data (tensor-borders of depth 2) and there are no noticeable improvements in the final surface if the degree is higher. Conversely guides based on single polynomials or lower-degree piecewise polynomial typically fail to capture the existing boundary data.

With this Ansatz, enforcing the  $C^1$  and  $C^2$  constraints in terms of the BB-coefficients leaves as free coefficients (shown as black bullets in Figure 13)

$$\mathbf{g}_{ijk,i+j+k=5}^* : \quad \mathbf{g}_{ijk}^0, j+k \leq 2, \quad \mathbf{g}_{ij0}^\ell, j=3,4,5, \quad \mathbf{g}_{122}^\ell, \mathbf{g}_{023}^\ell, \mathbf{g}_{032}^\ell.$$

That is, the center quadratic polynomial is to be determined and each sector has some extra degrees of freedom. For elliptic shapes, either the user should provide the location of the central point or we set it as the limit point of a subdivision scheme. To set the remaining free coefficients, we minimize the deviation of the guide from the boundary data in the sense of Figure 14: given the ct-map  $\rho$  and the tensor-border  $\mathbf{b}$ , we minimize

$$\min_{\text{free } \mathbf{g}_{ijk}^*} \|H(\mathbf{g} \circ \rho) - H(\mathbf{b})\|_2^2. \quad (4)$$

Guide creation and re-approximation can be alternated by using the preceding surface ring as boundary data  $\mathbf{b}$ .

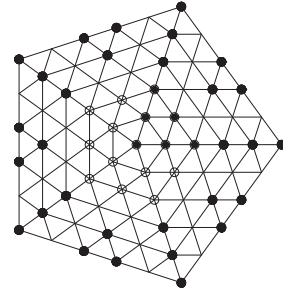


Figure 13: **Guide construction.** The free control points  $\mathbf{g}_{ijk}^\ell$  after enforcing  $C^2$  constraints between the polynomial pieces of degree 5 are marked as  $\bullet$ .

$$\min_{\text{free } \mathbf{g}_{ijk}} \left\| H \left( \begin{array}{c} \text{guide } \mathbf{g} \\ \triangle \times n \rightarrow \mathbb{R}^3 \end{array} \circ \begin{array}{c} \text{ct-map } \rho \\ S \times n \rightarrow \mathbb{R}^2 \end{array} \right) - H \left( \begin{array}{c} \text{tensor-border } \mathbf{b} \\ S \times n \rightarrow \mathbb{R}^3 \end{array} \right) \right\|$$

Figure 14: Derivation of a **default guide** surface for sprocket layout.  $H$  – Approximation operator (page 10)

## 5 A $C^2$ accelerated bi-3 guided subdivision

To illustrate the level of flexibility provided by guided surfacing, we consider a surface ring construction that samples with increasing density [KP08a]. We first consider the

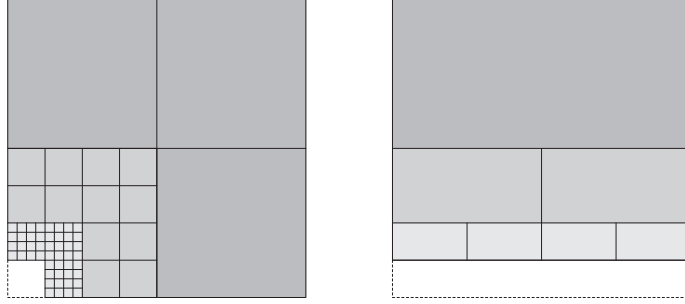


Figure 15: Structure of a sector of **accelerated  $C^2$  bi-3 subdivision**. (*left*) Quad-sprocket (Catmull-Clark) layout and (*right*) polar layout [KP08a].

sprocket (Catmull-Clark) layout Figure 15, *left*. At level  $m$ , each of the three quads of an L-shaped sector is partitioned into  $2^m \times 2^m$  subquads. The operator  $h^{33}$  (see page 11) is applied on each subquad, creating, after removal of the internal knots, a  $C^2$  bi-3 spline that joins  $C^2$  with its neighbor spline in the surface ring. The construction approximates the piecewise polynomial  $\mathbf{g} \circ \rho : [0..1]^2 \rightarrow \mathbb{R}$  by  $h^{33}$  up to second order at the corners of the  $34^m$  subquads of each quad-sprocket segment  $\mathbf{x}_\ell^m$ . For polar layout, there are  $2^m$  subquads (see Figure 15, *right*) and the construction approximates the piecewise polynomial up to second order at the corners of the  $2^m$  subquads of each polar segment  $\mathbf{x}_\ell^m$ . We call such schemes *accelerated*. To certify that the resulting subdivision surfaces are generically curvature continuous, [KP08a, Thm 6] tracked a sequence of local quadratic functions and showed their convergence to the quadratic Taylor expansion of  $\mathbf{g}$  at the central point.

Acceleration therefore circumvents one of the key assumptions that lead to the lower bounds on the degree of curvature continuous subdivision surfaces derived in [Rei96, Pra98]. Acceleration allows us to build  $C^2$  surfaces consisting of (infinitely many) polynomial pieces of degree (3,3), the continuity-and-degree combination hoped for since 1978 [CC78]. While the construction for the sprocket configurations seems hardly practical, acceleration for polar configurations is natural and has been turned

into a practical  $C^2$  bi-3 subdivision algorithm [Myl08].

**Acknowledgements.** The images were generated with the surface analysis tool *BezierView*. This work was supported by the National Science Foundation Grant 0728797.

## References

- [BR97] H. Bohl and U. Reif. Degenerate Bézier patches with continuous curvature. *Comput. Aided Geom. Design*, 14(8):749–761, 1997.
- [BSCB00] Marcelo Bertalmio, Guillermo Sapiro, Vicent Caselles, and Coloma Ballester. Image inpainting. In Kurt Akeley, editor, *Siggraph 2000, Computer Graphics Proceedings*, Annual Conference Series, pages 417–424. ACM Press / ACM SIGGRAPH / Addison Wesley Longman, 2000.
- [BW90] M. I. G. Bloor and M. J. Wilson. Using partial differential equations to generate free form surfaces. *Computer Aided Design, May 1990*, 22(4):202–212, 1990.
- [CC78] E. Catmull and J. Clark. Recursively generated B-spline surfaces on arbitrary topological meshes. *Computer-Aided Design*, 10:350–355, September 1978.
- [DMSB99] M. Desbrun, Mark Meyer, Peter Schröder, and Alan H. Barr. Implicit fairing of irregular meshes using diffusion and curvature flow. In Alyn Rockwood, editor, *Siggraph 1999*, Annual Conference Series, pages 317–324, Los Angeles, 1999. ACM Siggraph, Addison Wesley Longman.
- [Flo97] Michael S. Floater. Parametrization and smooth approximation of surface triangulations. *Computer Aided Geometric Design*, 14(3):231–250, 1997.
- [GGH02] Xianfeng Gu, Steven J. Gortler, and Hugues Hoppe. Geometry images. In John Hughes, editor, *SIGGRAPH 2002 Conference Proceedings*, Annual Conference Series, pages 335–361. ACM Press/ACM SIGGRAPH, 2002.
- [GH89] John A. Gregory and Jörg M. Hahn. A  $C^2$  polygonal surface patch. *Comput. Aided Geom. Design*, 6(1):69–75, 1989.
- [GH95] C. M. Grimm and J. F. Hughes. Modeling surfaces of arbitrary topology using manifolds. *Computer Graphics*, 29(Annual Conference Series):359–368, 1995.
- [Gre94] G. Greiner. Variational design and fairing of spline surfaces. *Computer Graphics Forum*, 13(3):C/143–C/154, 1994.
- [GZ99] John A. Gregory and Jianwei Zhou. Irregular  $C^2$  surface construction using bi-polynomial rectangular patches. *Comput. Aided Geom. Design*, 16(5):423–435, 1999.



- [Hah89] Jörg Hahn. Filling polygonal holes with rectangular patches. In *Theory and practice of geometric modeling (Blaubeuren, 1988)*, pages 81–91. Springer, Berlin, 1989.
- [HG00] Andreas Hubeli and Markus Gross. Fairing of non-manifolds for visualization. In *Proceedings Visualization 2000*, pages 407–414. IEEE Computer Society Technical Committee on Computer Graphics, 2000.
- [HP07] Klaus Hildebrandt and Konrad Polthier. Constraint-based fairing of surface meshes. In Alexander Belyaev and Michael Garland, editors, *SGP07: Eurographics Symposium on Geometry Processing*, pages 203–212. Eurographics Association, 2007.
- [JKL<sup>+</sup>] Miao Jin, Juhno Kim, Feng Luo, Seungyong Lee, and Xianfeng Gu. Conformal surface parameterization using Euclidean Ricci flow. *Technical Report*. [http://www.cise.ufl.edu/~gu/publications/technical\\_report.htm](http://www.cise.ufl.edu/~gu/publications/technical_report.htm).
- [KCVS98] Leif Kobbelt, Swen Campagna, Jens Vorsatz, and Hans-Peter Seidel. Interactive multi-resolution modeling on arbitrary meshes. In Michael Cohen, editor, *SIGGRAPH 98 Conference Proceedings*, pages 105–114. ACM SIGGRAPH, Addison Wesley, July 1998.
- [KHPS97] L. Kobbelt, T. Hesse, H. Prautzsch, and K. Schweizerhof. Interactive mesh generation for FE-computation on free form surfaces. *Engng. Comput.*, 14:806–820, 1997.
- [Kim97] Ron Kimmel. Intrinsic scale space for images on surfaces: The geodesic curvature flow. *Graphical models and image processing: GMIP*, 59(5):365–372, September 1997.
- [KMP06] K. Karčiauskas, A. Myles, and J. Peters. A  $C^2$  polar jet subdivision. In A. Scheffer and K. Polthier, editors, *Proceedings of Symposium of Graphics Processing (SGP), June 26-28 2006, Cagliari, Italy*, pages 173–180. ACM Press, 2006.
- [Kob97] L. Kobbelt. Discrete fairing. In Tim Goodman and Ralph Martin, editors, *Proceedings of the 7th IMA Conference on the Mathematics of Surfaces (IMA-96)*, volume VII of *Mathematics of Surfaces*, pages 101–130, Winchester, UK, September 1997. Information Geometers.
- [KP07a] K. Karčiauskas and J. Peters. Concentric tessellation maps and curvature continuous guided surfaces. *Computer-Aided Geometric Design*, 24(2):99–111, Feb 2007.
- [KP07b] K. Karčiauskas and J. Peters. Guided  $C^2$  spline surfaces with V-shaped tessellation. In J. Winkler and R. Martin, editors, *Mathematics of Surfaces*, pages 233–244, 2007.

- [KP07c] K. Karčiauskas and J. Peters. Parameterization transition for guided  $C^2$  surfaces of low degree. In *Sixth AFA Conference on Curves and Surfaces Avignon, June 29-July 5, 2006*, pages 183–192, April 2007.
- [KP07d] Kęstutis Karčiauskas and Jörg Peters. Bicubic polar subdivision. *ACM Trans. Graph.*, 26(4):14, 2007.
- [KP08a] K. Karčiauskas and J. Peters. Guided subdivision. Technical Report 2008-464, Dept CISE, University of Florida, 2008. posted since 2005 at <http://www.cise.ufl.edu/research/SurfLab/papers.shtml>.
- [KP08b] K. Karčiauskas and J. Peters. On the curvature of guided surfaces. *Computer Aided Geometric Design*, 25(2):69–79, feb 2008.
- [KP09a] K. Karčiauskas and J. Peters. Assembling curvature continuous surfaces from triangular patches. *SMI 26/105, Computers and Graphics*, 2009. <http://dx.doi.org/10.1016/j.cag.2009.03.015>.
- [KP09b] K. Karčiauskas and J. Peters. Finite curvature continuous polar patches. In E. Hancock and R.R. Martin, editors, *IMA Mathematics of Surfaces XIII Conference*, pages xx–xx, 2009. in press.
- [KP09c] K. Karčiauskas and J. Peters. Lens-shaped surfaces and  $C^2$  subdivision. *Computing*, 2009. to appear.
- [KPN1] K. Karčiauskas and J. Peters. Guided spline surfaces. *Computer Aided Geometric Design*, pages 1–20, 2009 N1.
- [KPR04] K. Karčiauskas, J. Peters, and U. Reif. Shape characterization of subdivision surfaces – case studies. *Computer-Aided Geometric Design*, 21(6):601–614, july 2004.
- [Lev06] Adi Levin. Modified subdivision surfaces with continuous curvature. *ACM Transactions on Graphics*, 25(3):1035–1040, July 2006.
- [Loo87] C. Loop. *Smooth Subdivision Surfaces Based on Triangles*. PhD thesis, Mathematics, University of Utah, 1987.
- [Loo04] Charles Loop. Second order smoothness over extraordinary vertices. In *Symp Geom Processing*, pages 169–178, 2004.
- [LS08] Charles T. Loop and Scott Schaefer.  $G^2$  tensor product splines over extraordinary vertices. *Comput. Graph. Forum*, 27(5):1373–1382, 2008.
- [MDSB02] M. Meyer, M. Desbrun, P. Schroder, and A.H. Barr. Discrete differential-geometry operators for triangulated 2-manifolds. *Visualization and Mathematics*, 3:34–57, 2002.
- [MKP07] Ashish Myles, Kęstutis Karčiauskas, and Jörg Peters. Extending Catmull-Clark subdivision and PCCM with polar structures. In *PG '07: Proceedings of the 15th Pacific Conference on Computer Graphics and Applications*, pages 313–320, Washington, DC, USA, 2007. IEEE Comp Soc.

- [MKP08] Ashish Myles, Kęstutis Karčiauskas, and Jörg Peters. Pairs of bi-cubic surface constructions supporting polar connectivity. *Comput. Aided Geom. Des.*, 25(8):621–630, 2008.
- [dC92] M.P. do Carmo. *Riemannian Geometry*. Birkhäuser Verlag, Boston, 1992.
- [MS92] Henry P. Moreton and Carlo H. Séquin. Functional optimization for fair surface design. *Computer Graphics*, 26(2):167–176, July 1992.
- [MS96] R. Malladi and J. A. Sethian. Flows under min/max curvature flow and mean curvature: applications in image processing. *Lecture Notes in Computer Science*, 1064:pp251, 1996.
- [Myl08] Ashish Myles. *Curvature-continuous Bicubic Subdivision Surfaces for Polar Configurations*. PhD thesis, Dept CISE, U Florida, USA, 2008.
- [NG00] J. Cotrina Navau and N. Pla Garcia. Modeling surfaces from meshes of arbitrary topology. *Comput. Aided Geom. Design*, 17(7):643–671, 2000.
- [Pet96] J. Peters. Curvature continuous spline surfaces over irregular meshes. *Computer-Aided Geometric Design*, 13(2):101–131, Feb 1996.
- [Pet02] J. Peters.  $C^2$  free-form surfaces of degree (3,5). *Computer-Aided Geometric Design*, 19(2):113–126, 2002.
- [PP93] Ulrich Pinkall and Konrad Polthier. Computing discrete minimal surfaces and their conjugates. *Experimental Mathematics*, 2(1):15–36, 1993.
- [PR04] J. Peters and U. Reif. Shape characterization of subdivision surfaces – basic principles. *Computer-Aided Geometric Design*, 21(6):585–599, july 2004.
- [PR08] J. Peters and U. Reif. *Subdivision Surfaces*, volume 3 of *Geometry and Computing*. Springer-Verlag, New York, 2008.
- [Pra97] H. Prautzsch. Freeform splines. *Computer Aided Geometric Design*, 14(3):201–206, 1997.
- [Pra98] Hartmut Prautzsch. Smoothness of subdivision surfaces at extraordinary points. *Adv. Comput. Math.*, 9(3-4):377–389, 1998.
- [PU00] H. Prautzsch and G. Umlauf. Triangular  $G^2$ splines. In L.L. Schumaker P.J. Laurent, A. LeMéhauté, editor, *Curve and Surface Design*, pages 335–342. Vanderbilt University Press, 2000.
- [Rei96] U. Reif. A degree estimate for subdivision surfaces of higher regularity. *Proc. Amer. Math. Soc.*, 124(7):2167–2174, 1996.
- [Rei98] U. Reif. TURBS—topologically unrestricted rational  $B$ -splines. *Constructive Approximation*, 14(1):57–77, 1998.

- [Rei99] Ulrich Reif. *Analyse und Konstruktion von Subdivisionsalgorithmen für Freiformflächen beliebiger Topologie*. Shaker Verlag, Aachen, 1999.
- [Sap94] Sapidis, N. *Designing Fair Curves and Surfaces*. SIAM, Philadelphia, 1994.
- [SdS00] A. Sheffer and E. de Sturler. Surface parameterization for meshing by triangulation flattening. *Proc. 9th International Meshing Roundtable*, pages 161–172, 2000.
- [SK00] R. Schneider and L. Kobbelt. Generating fair meshes with  $G^1$  boundary conditions. In Ralph Martin and Wenping Wang, editors, *Proceedings of the Conference on Geometric Modeling and Processing (GMP-00)*, pages 251–261, Los Alamitos, April 10–12 2000. IEEE.
- [Sur] <http://www.cise.ufl.edu/research/SurfLab/>.
- [Tau95] Gabriel Taubin. A signal processing approach to fair surface design. In Robert Cook, editor, *SIGGRAPH 95 Conference Proceedings*, Annual Conference Series, pages 351–358. ACM SIGGRAPH, Addison Wesley, August 1995. held in Los Angeles, California, 06-11 August 1995.
- [VR97] Tamás Várady and Alyn Rockwood. Geometric construction for setback vertex blending. *Computer-aided Design*, 29(6):413–425, 1997.
- [WJE00] Rüdiger Westermann, Christopher Johnson, and Thomas Ertl. A level-set method for flow visualization. In T. Ertl, B. Hamann, and A. Varshney, editors, *Proceedings Visualization 2000*, pages 147–154. IEEE Computer Society Technical Committee on Computer Graphics, 2000.
- [WW92] William Welch and Andrew Witkin. Variational surface modeling. *Computer Graphics (SIGGRAPH '92 Proceedings)*, 26(2):157–166, July 1992.
- [WW94] William Welch and Andrew Witkin. Free-Form shape design using triangulated surfaces. In Andrew Glassner, editor, *Proceedings of SIGGRAPH '94 (Orlando, Florida, July 24–29, 1994)*, pages 247–256. ACM SIGGRAPH, ACM Press, July 1994.
- [Ye97] Xiuzi Ye. Curvature continuous interpolation of curve meshes. *Computer Aided Geometric Design*, 14(2):169–190, 1997.
- [YZ04] Lexing Ying and Denis Zorin. A simple manifold-based construction of surfaces of arbitrary smoothness. *ACM TOG*, 23(3):271–275, August 2004.
- [ZS01] Denis Zorin and Peter Schröder. A unified framework for primal/dual quadrilateral subdivision schemes. *Comput. Aided Geom. Design*, 18(5):429–454, 2001. Subdivision algorithms (Schloss Dagstuhl, 2000).